Science

AAAS

Neodymium-142 Evidence for Hadean Mafic Crust
Jonathan O'Neil, *et al.*
Science **321**, 1828 (2008);
DOI: 10.1126/science.1161925

ple closely matching our simulation results. There, regularly spaced vent sites, with black smokers venting fluids close to 400°C, have been active for several years (*34*, *35*). Magnetic anomaly data show that upflow zones are narrow pipelike structures that reach to a depth of at least a few hundreds of meters and possibly to the base of the hydrothermal system with a regular spacing comparable with that in our simulations (*3*). Though natural systems are geologically much more complex than the numerical model described here, we suggest that the MEF is likely to operate in a state of maximum energy transport, with recharge occurring close to the vent sites. The optimal site for future in situ tracer injection experiments would therefore be about twice the radius of a black smoker vent field. The relatively short residence times resulting from our calculations also indicate that such an experiment can lead to a successful tracer test within a realistic time frame.

Massive sulfide ore deposits form when convecting seawater leaches metals from new basaltic crust and reprecipitates them as sulfides at the outflow points of active black smokers. The solubility of iron, zinc, and copper increases almost exponentially with temperature (*36*). Our simulations indicate that the average temperature of fluid-rock interaction is much higher than would be expected from dispersed seawater infiltration across the spreading axis (*37*). As a result, solubility-limited leaching is expected to be much more effective by including large parts of the hot downflow path and not being restricted to the basal reaction zone of the system. With an average copper content in mid-ocean ridge basalt of 25 parts per million, a typical small seafloor sulfide deposit of 0.2 million metric tons containing 3% copper (*38*) can be formed by leaching only the upflow zone and its immediately surrounding hot downflow zone. The copper solubility in this region varies from $\sim 10^{-7}$ mol/kg at 200°C to $\sim 10^{-4}$ mol/kg at 350°C, ensuring that the metals are quickly leached and a deposit can form within a period of 100 to 1000 years.

References and Notes

1. C. Stein, S. Stein, *J. Geophys. Res.* **99**, 3081 (1994).
2. A. Fisher, in *Energy and Mass Transfer in Marine Hydrothermal Systems*, P. E. Halbach, V. Tunnicliffe, J. R. Hein, Eds. (Dahlem Univ. Press, Berlin, 2003), vol. 89, pp. 29–52.
3. M. Tivey, H. Johnson, *Geology* **30**, 979 (2002).
4. L. Coogan et al., *Am. J. Sci.* **306**, 389 (2006).
5. H. Johnson, K. Becker, R. Von Herzen, *Geophys. Res. Lett.* **20**, 1875 (1993).
6. S. Kelley, J. Baross, J. Delaney, *Annu. Rev. Earth Planet. Sci.* **30**, 385 (2002).
7. P. Nehlig, T. Juteau, *Mar. Geol.* **84**, 209 (1988).
8. W. Wilcock, A. Fisher, *Geophys. Monogr.* **144**, 51 (2004).
9. M. Tolstoy, F. Waldhause, D. Bohnenstiehl, R. Weekly, W. Kim, *Nature* **451**, 181 (2008).
10. S. Ingebritsen, D. O. Hayba, *Geophys. Res. Lett.* **21**, 2199 (1994).
11. T. Jupp, A. Schultz, *Nature* **403**, 880 (2000).
12. D. Coumou, T. Driesner, S. Geiger, C. Heinrich, S. Matthai, *Earth Planet. Sci. Lett.* **245**, 218 (2006).
13. B. Travis, D. Janecky, N. Rosenberg, *Geophys. Res. Lett.* **18**, 1441 (1991).
14. M. Rabinowicz, J. Boulegue, P. Genthon, *J. Geophys. Res.* **103**, 24045 (1998).
15. M. Rabinowicz, J. Sempéré, P. Genthon, *J. Geophys. Res.* **104**, 29275 (1999).
16. F. Fontaine, M. Rabinowicz, J. Boulegue, *Earth Planet. Sci. Lett.* **184**, 407 (2001).
17. S. Ingebritsen, W. Sanford, C. Neuzil, *Groundwater in Geologic Processes* (Cambridge Univ. Press, Cambridge, ed. 2, 2006).
18. G. Haar, Kell, *NBS/NRC Steam Tables* (Hemisphere Publishing, New York, 1984).
19. D. Coumou, thesis, Eidgenössische Technische Hochschule–Zurich, Switzerland (2008).
20. U. Ginster, M. Mottl, R. Von Herzen, *J. Geophys. Res.* **99**, 4937 (1994).
21. E. Baker, T. Urabe, *J. Geophys. Res.* **101**, 8685 (1996).
22. P. Ramondenc, L. Germanovich, K. Von Damm, R. Lowell, *Earth Planet. Sci. Lett.* **245**, 487 (2006).
23. Materials and methods are available as supporting material on *Science* Online.
24. J. Sinton, R. Detrick, *J. Geophys. Res.* **97**, 197 (1992).
25. R. Lowell, A. Rona, R. Von Herzen, *J. Geophys. Res.* **100**, 327 (1995).
26. F. Fontaine, W. Wilcock, *Geochem. Geophys. Geosyst.* **8**, Q07010 (2007).
27. D. Kadko, D. Butterfield, *Geochim. Cosmochim. Acta* **62**, 1521 (1998).
28. D. Kadko, G. K., D. Butterfield. *Geochim. Cosmochim. Acta* **71**, 6019 (2007).
29. C. Lister, *Geophys. J. Int.* **120**, 45 (1995).
30. T. Jupp, A. Schultz, *J. Geophys. Res.* **109**, 10.1029/2003JB002697 (2004).
31. W. Malkus, *Proc. R. Soc. London. Ser. A* **225**, 196 (1954).
32. F. Busse, D. Joseph, *J. Fluid Mech.* **54**, 521 (1972).
33. W. S. D. Wilcock, *J. Geophys. Res.* **103**, 2585 (1998).
34. E. M. Van Ark et al., *J. Geophys. Res.* **112**, 10.1029/2005JB004210 (2007).
35. D. Glickson, D. Kelley, J. Delaney, *Geochem. Geophys. Geosyst.* **8**, Q06010 (2007).
36. J. Hemley, G. Cygan, J. Fein, G. Robinson, W. Angelo, *Econ. Geol.* **87**, 1 (1992).
37. J. Franklin, H. Gibson, I. Jonasson, A. Galley, in *Economic Geology, 100th Anniversary Volume*, J. W. Hedenquist, J. F. H. Thompson, R. J. Goldfarb, J. P. Richards, Eds. (Society of Economic Geologists, Littleton, CO, 2005), pp. 523–560.
38. M. Hannington, I. Jonasson, P. Herzig, S. Petersen, *Geophys. Monogr.* **91**, 115 (1995).
39. This work was supported by the Swiss National Science Foundation (grant 200020-107955). The authors thank S. Geiger for providing the mesh depicted in Fig. 1 and S. Ingebritsen, P. Weiss, L. Cathles, and three anonymous reviewers for useful discussions as well as careful proofreading of earlier versions of the manuscript.

Neodymium-142 Evidence for Hadean Mafic Crust

Jonathan O'Neil,[1]* Richard W. Carlson,[2] Don Francis,[1] Ross K. Stevenson[3]

Neodymium-142 data for rocks from the Nuvvuagittuq greenstone belt in northern Quebec, Canada, show that some rock types have lower $^{142}Nd/^{144}Nd$ ratios than the terrestrial standard ($\varepsilon^{142}Nd = -0.07$ to -0.15). Within a mafic amphibolite unit, $^{142}Nd/^{144}Nd$ ratios correlate positively with Sm/Nd ratios and produce a ^{146}Sm-^{142}Nd isochron with an age of 4280^{+53}_{-81} million years. These rocks thus sample incompatible-element-enriched material formed shortly after Earth formation and may represent the oldest preserved crustal section on Earth.

The past decade has seen dramatic discoveries concerning the oldest rocks on Earth, with precise zircon ages pushing the terrestrial rock record back beyond 4 billion years ago (Ga) (*1*) and the detrital zircon record to beyond 4.3 Ga (*2*). Because zircon is a rare to non-existent phase in most mafic rocks, prospecting for ancient crust through zircon analysis has focused the search on the more evolved rock types that likely, as today, do not represent the major volume of Earth's crust.

The short-lived ^{146}Sm-^{142}Nd isotopic system [half life ($T_{1/2}$) = 103 million years (My)] has proven useful for investigating the early differentiation of the silicate portion of Earth. Recent measurements of the ^{146}Sm-^{142}Nd system in Eoarchean (4.0 to 3.6 Ga) rocks, primarily from Greenland, show excesses in $^{142}Nd/^{144}Nd$ ratios of 10 to 20 parts per million (ppm) compared to modern terrestrial standards testifying to Earth differentiation events within a few tens of million years of Earth formation (*3*–*7*). The high $^{142}Nd/^{144}Nd$ measured for these rocks indicate that the Eoarchean crustal rocks were sourced in a mantle with high Sm/Nd ratio. We describe evidence from the Nuvvuagittuq greenstone belt that a complimentary, low Sm/Nd ratio, reservoir is also found in the terrestrial rock record and that these rocks may be the oldest yet discovered on Earth.

The recent discovery of the Nuvvuagittuq greenstone belt in Ungava, Québec, provides a new suite of Eoarchean rocks with which to further our understanding of the early crust-mantle system. The Nuvvuagittuq belt exposes volcanic and metasedimentary rocks in an isoclinal synform refolded into a more open south-plunging synform (Fig. 1) (*8*) and is surrounded by a 3.66-billion-

[1]Earth and Planetary Sciences Department, McGill University, 3450 University Street, Montreal, Quebec, H3A 2A7, Canada. [2]Department of Terrestrial Magnetism, Carnegie Institution of Washington, 5241 Broad Branch Road, NW, Washington, DC 20015, USA. [3]GEOTOP (Centre de recherche en géochemie et géodynamique), Université du Québec à Montréal, Post Office Box 8888, Succursale Centre-ville, 210, Président-Kennedy Avenue, Montreal, Quebec H3C 3P8, Canada.

*To whom correspondence should be addressed. E-mail: oneil_jo@eps.mcgill.ca

year (Gy) tonalite (*9, 10*). Geochronological constraints for the belt come mainly from rare felsic bands (0.5 to 1 m in width) composed of plagioclase, biotite, and quartz that have yielded a discordant zircon age of 3817 ± 16 My (*9*). A minimum age of 3750 My has also been obtained from U-Pb ion microprobe analyses of zircons found in a similar lithology (*11*). Although no clear crosscutting relationship has been found, the felsic bands are commonly found within gabbroic sills that may suggest an intrusive nature for these rocks. The dominant lithology of the belt is a cummingtonite-amphibolite referred to as "faux-amphibolite" because of its unusual mineralogical composition in which the dominant amphibole is cummingtonite, in contrast to the hornblende-dominated amphibolites usually found in the Superior Province. The faux-amphibolite is composed of variable amounts of cummingtonite, plagioclase, biotite, and quartz plus or minus garnet (*8*), commonly with compositional layering defined by the alternation of biotite-rich and cummingtonite-rich laminations. These rocks are very heterogeneous and can be almost entirely composed of cummingtonite, giving them a light gray color, whereas some are reddish brown in color and mainly consist of biotite and garnet, with minor amounts of cummingtonite.

The faux-amphibolite is intruded in the western limb of the synform by ultramafic and gabbroic sills. Compared with these relatively undeformed gabbros, two larger gabbroic sills toward the center of the belt display pronounced gneissic textures, suggesting that they may be older than the less-deformed gabbroic sills. The faux-amphibolite in the western limb rarely contains garnet, whereas toward the center of the belt it has abundant garnet and commonly higher Al_2O_3 contents (*8*). The faux-amphibolite was originally interpreted to be a paragneiss (*10*) because of the abundance of garnet and compositional layering. These rocks, however, are more mafic than typical Archean shales and have a basaltic major element composition similar to those of the gabbroic sills but with lower CaO, slightly lower TiO_2, and commonly higher Al_2O_3 contents. These features suggested that they could be highly altered mafic pyroclastites comagmatic with the gabbro sills (*8*). The faux-amphibolite, however, is enriched in light rare earth elements (LREEs), which argues against a direct cogenetic relationship with the gabbros that intrude it, all of which have flat REE patterns (table S1).

Seven samples of the faux-amphibolite yielded low $^{147}Sm/^{144}Nd$ ratios (0.143 to 0.179) with correspondingly low measured $^{143}Nd/^{144}Nd$ ($\varepsilon^{143}Nd$ from −27.4 to −9.7, where $\varepsilon^{143}Nd$ = $[(^{143}Nd/^{144}Nd)_{sample}/(^{143}Nd/^{144}Nd)_{CHUR} − 1] \times 10^4$ and CHUR is chondritic uniform reservoir) and $^{142}Nd/^{144}Nd$ ratios ($\varepsilon^{142}Nd$ = −0.07 to −0.15, where $\varepsilon^{142}Nd$ = $[(^{142}Nd/^{144}Nd)_{sample}/(^{142}Nd/^{144}Nd)_{standard}] − 1] \times 10^4$) relative to the terrestrial standard [Fig. 2, table S2, and supporting online material (SOM) text]. Two tonal-

ite samples also show low $^{142}Nd/^{144}Nd$ ($\varepsilon^{142}Nd$ = −0.12 to −0.16) as do both felsic band samples ($\varepsilon^{142}Nd$ = −0.09 to −0.10), although the felsic bands overlap the terrestrial standard within the external error of 0.06 as determined by the 2σ-population reproducibility of the standards (SOM text). The gabbros have $^{147}Sm/^{144}Nd$ ratios (0.183 to 0.193) and measured $^{143}Nd/^{144}Nd$ ratios ($\varepsilon^{143}Nd$ = −4.7 to 0.6) that are just slightly below chondritic values, with $^{142}Nd/^{144}Nd$ ratios overlapping the terrestrial standard ($\varepsilon^{142}Nd$ = −0.09 to −0.02).

The Nuvvuagittuq rocks have $^{142}Nd/^{144}Nd$ ratios that fall between the $^{142}Nd/^{144}Nd$ ratios of chondrites and the terrestrial standard [e.g., (*12*)]. This is in contrast to Eoarchean rocks of Greenland that have $^{142}Nd/^{144}Nd$ values higher than the terrestrial standard (*3–7*). Also, unlike the Greenland rocks, the $^{142}Nd/^{144}Nd$ ratios of the gabbros and faux-amphibolite correlate positively with their Sm/Nd ratios, producing a statistically significant slope corresponding to a $^{146}Sm/^{144}Sm$ ratio of 0.00116 ± 0.00049 [mean square weighted deviation (MSWD) = 0.67, error with 95% confidence] and an initial $\varepsilon^{142}Nd$ = −0.02 ± 0.15 relative to the terrestrial standard (Fig. 3). This line is fit assigning a constant ±6 ppm error for $^{142}Nd/^{144}Nd$ for all samples to represent the external reproducibility of these isotope ratio determinations. For a solar system initial

$^{146}Sm/^{144}Nd$ = 0.008 (*13*) at 4567 Ga (*14*), this slope corresponds to an age of 4280^{+53}_{-81} My. Fitting just the faux-amphibolite data provides a slope of 0.0012 ± 0.0011 corresponding to an age of 4286^{+96}_{-370} My with an initial $\varepsilon^{142}Nd$ = +0.02 ± 0.32 relative to the terrestrial standard. Both the tonalites and the felsic bands fall off these correlations to the low Sm/Nd ratio side.

At the whole-rock scale, isochrons need not provide the crystallization ages of the rocks that define the isochron. Because 4.28-Gy-old the isochron shown in Fig. 3 goes through the value of the modern terrestrial mantle, the unfractionated rocks would plot close to the modern mantle value on Fig. 3 regardless of their age. For example, 12 ultramafic to gabbroic samples from one sill cutting the faux-amphibolite give a $^{147}Sm-^{143}Nd$ isochron age of 3840 ± 280 My (MSWD = 3.8) with initial $\varepsilon^{143}Nd$ = +0.9 (Fig. 4A), but the data for some of the same samples lie close to the 4.28-Gy isochron in Fig. 3. The old age in Fig. 3 is dictated by the low Sm/Nd ratios of the faux-amphibolite. The faux-amphibolite defines a scattered $^{147}Sm-^{143}Nd$ correlation with an age of 3819 ± 270 My (MSWD = 5.5) and an initial $\varepsilon^{143}Nd$ = −1.4. The negative initial $\varepsilon^{143}Nd$ of the faux-amphibolites is unusual for rocks of this age but is consistent with the low $^{142}Nd/^{144}Nd$ ratios measured for these samples.
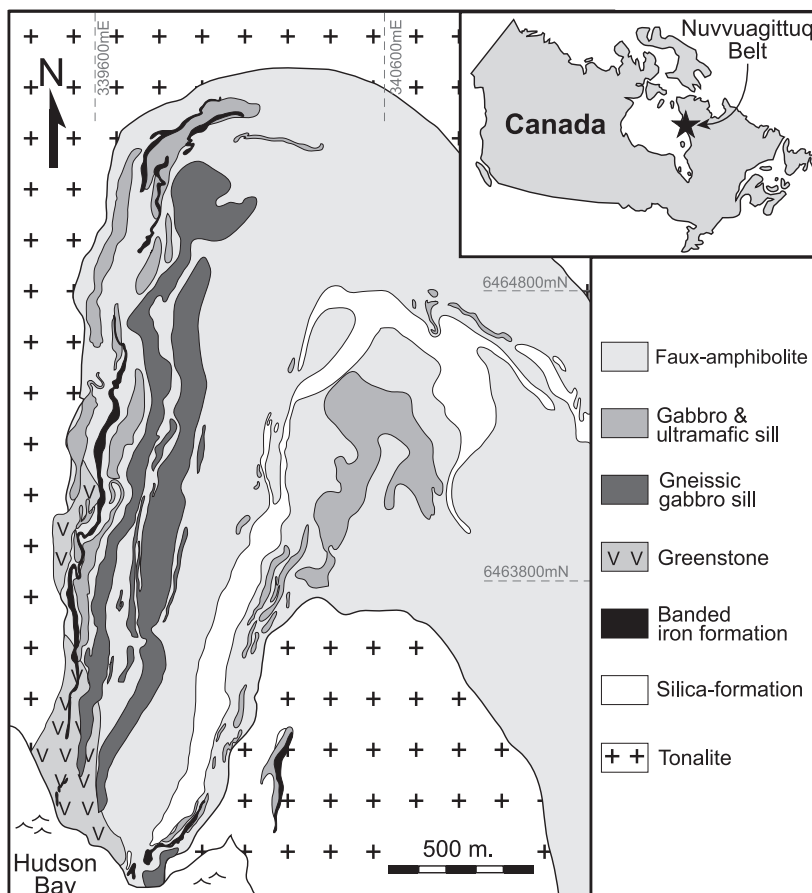
Fig. 1. Simplified geological map of the Nuvvuagittuq greenstone belt. The geology of the belt is described in more detail in (*8*). Coordinates are in universal transverse mercator zone 18 NAD 27.

Sm/Nd ratios as low as those measured in the faux-amphibolite and felsic bands would not produce $^{142}Nd/^{144}Nd$ ratios outside of measurement uncertainty from the terrestrial standard if this parent/daughter fractionation occurred later than ~4.1 to 4.2 Ga. Thus, even if the faux-amphibolite has crystallization ages of 3.8 Gy, the steepness of the $^{142}Nd/^{144}Nd$–Sm/Nd covariation requires that they sample a LREE-enriched material that is at least 4.28 Gy old. This LREE-enriched component could be either older crust that contaminated parental melts like the gabbros or a LREE-enriched mantle source that melted to produce the faux-amphibolite. Regardless of the nature of the LREE-enriched component, its low Sm/Nd ratio must have formed while ^{146}Sm was still extant, and the 4.28-Gy-old isochron provides the best indication of the age of this end member.

An alternate interpretation is that the 4.28-Gy-old isochron indeed dates the formation age of the faux-amphibolite, but this possibility is not supported by the 3.8-Gy-old ^{147}Sm-^{143}Nd age of this unit. For an isochron that passes through the terrestrial mantle point, however, a reduction in Sm/Nd ratio of the faux-amphibolite with the lowest Sm/Nd ratios by only 4.4% caused by metamorphism at 3.8 Ga would rotate a ^{147}Sm-^{143}Nd isochron of 4.28 Gy to 3.8 Gy. Increasing the Sm/Nd ratio of the low–Sm/Nd ratio faux-amphibolite by 4.4% would increase the ^{146}Sm-^{142}Nd isochron age by only 25 My, well within the uncertainty of the data, illustrating the potential of the ^{146}Sm-^{142}Nd system to see through later metamorphic events.

Obviously, other corroborative data would help resolve whether the 4.28-Gy age dates the rocks themselves or an older component involved in their genesis. In spite of attempts to do so, zircons have not yet been found in the faux-amphibolite. Whole-rock Pb isotope data for the faux-amphibolite (table S1) do not define a valid isochron. The best fit line through the $^{206}Pb/^{204}Pb$–$^{207}Pb/^{204}Pb$ data corresponds to an age of 2.4 ± 0.4 Gy, indicative of a late disturbance of the U-Pb system at the whole-rock scale. The faux-amphibolite is crosscut by the gabbro sills and therefore must be older than the gabbros. Although the undeformed gabbros give a ^{147}Sm-^{143}Nd isochron age of 3.84 Gy (Fig. 4A), an isochron constructed from nine samples of the more gneissic, presumably older, gabbros gives an age of 4023 ± 110 My (MSWD = 0.78) with initial $\varepsilon^{143}Nd$ = +1.7 (Fig. 4B). All samples of the faux-amphibolite, except PC-129, yield negative $\varepsilon^{143}Nd$(3.8 Gy) values ranging from –3.2 to –1.0, compared with the mostly positive $\varepsilon^{143}Nd$(3.8 Ga) (–0.2 to +3.1) for the gabbro and ultramafic sills (table S2). When the $\varepsilon^{143}Nd$ values for the faux-amphibolite, except PC-129, are calculated for an age of 4.28 Gy, they range from – 0.3 to +2.3 with an average value of 0.6. This average initial $\varepsilon^{143}Nd$ value is consistent with the mantle value at 4.28 Ga predicted by various depleted mantle evolution models (5, 15, 16), but

Fig. 2. The $^{142}Nd/^{144}Nd$ ratios for the Nuvvuagittuq rocks normalized to the La Jolla standard. Gray solid bar corresponds to the external (6 ppm) error obtained on the terrestrial standard. Error bars for individual samples correspond to either the 2σ-mean internal precision of the mass spectrometer analysis or the 2σ-mean of repeat analysis of the sample on the same mass spectrometer filament load. Solid circle indicates ultramafic sill; open circles, gabbro; diamonds, faux-amphibolite (alternating open and solid diamonds show data for replicate analyses of single samples); squares, tonalite; and triangles (alternating open and solid triangles show data for replicate analyses of single samples), felsic band.
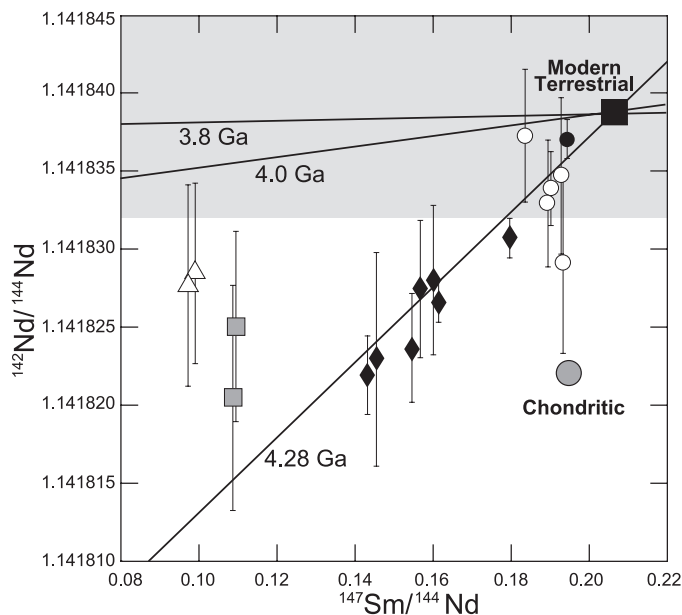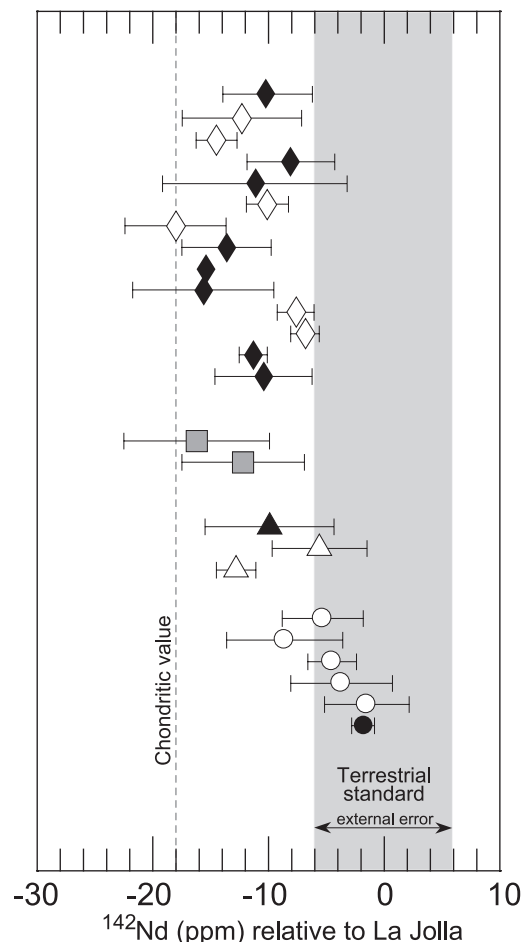

Fig. 3. $^{142}Nd/^{144}Nd$ versus $^{147}Sm/^{144}Nd$ isochron diagram. Symbols as described for Fig. 2. Only the average value of replicate analyses is plotted on this figure. The horizontal gray band shows the ±6 ppm external precision obtained on the terrestrial standard. Error bars on individual samples are either the 2σ mean of multiple analyses or the 2σ mean of the individual mass spectrometer run for samples run only once. The best fit line through the faux-amphibolite and gabbro data corresponding to an age of 4.28 Gy is shown, as are 3.8- and 4.0-Gy isochrons for reference. The gray circle shows the average value measured for ordinary and enstatite chondrites (12).

Fig. 4. ^{147}Sm-^{143}Nd isochron diagrams. (**A**) Ultramafic to gabbroic samples from one differentiated sill. (**B**) Samples from the gabbro sills that show a strong gneissic metamorphic texture.
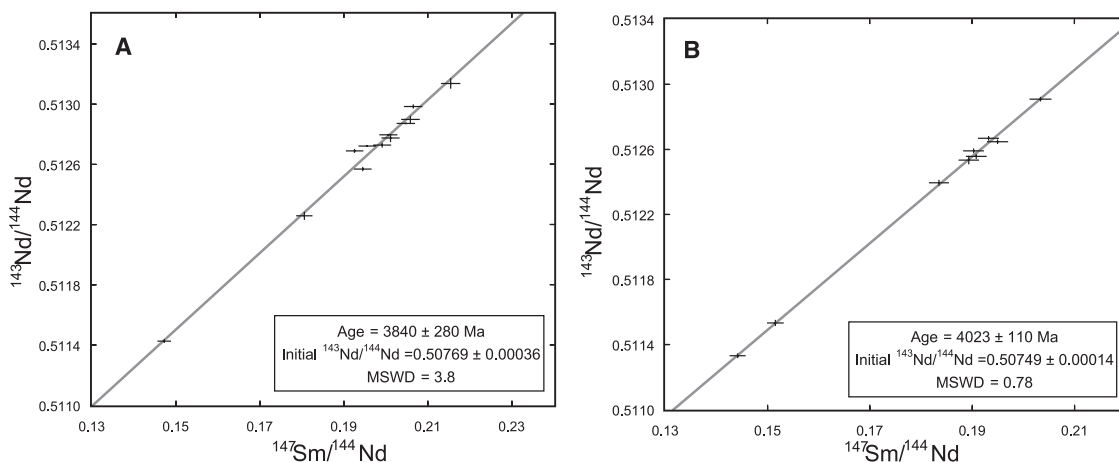
perhaps not as depleted as suggested by the Greenland data (*7, 17, 19*). As a result, the calculated ^{143}Nd depleted-mantle model ages (T_{DM}) for the faux-amphibolite, except PC-129, range from 4.1 to 4.4 Ga, consistent with the age suggested by ^{142}Nd systematics and in contrast to the 3.2 to 3.6 Ga T_{DM} values of the gabbros and sample PC-129 (table S2).

Whether or not the faux-amphibolite is 4.28 Gy old, its compositional characteristics may provide clues to the process of crust formation in the Hadean (>4.0 Ga). The basaltic major and compatible (e.g., Ni) trace element composition of the faux-amphibolite is consistent with derivation from a peridotitic mantle. Compared to the gabbros and to modern mid-ocean ridge basalts, the most unusual compositional characteristic of the faux-amphibolite is its low Ca content, high K and Rb contents, and LREE enrichment. Because elements like K and Rb are easily affected by alteration, however, it is unclear whether these are magmatic features of the faux-amphibolite. The LREE enrichment could reflect relatively low degrees of mantle melting, but this explanation is not supported by the relatively low concentration of elements such as Ti and Nb in the faux-amphibolite. The high LREE to Nb ratios of the faux amphibolite, however, is similar to that of modern calc-alkaline melts produced in convergent margin settings. The Hadean crust, represented by the faux-amphibolite, was intruded at 4.0 and 3.8 Ga by gabbro and ultramafic sills that have the ^{143}Nd and ^{142}Nd isotopic composition of the depleted mantle at the time of their intrusion. The low ^{142}Nd/^{144}Nd ratios of tonalites and felsic bands that were emplaced between 3.8 and 3.6 Ga, well after ^{146}Sm was extinct (*9–11*), suggest that they formed by the partial melting of the faux-amphibolite.

References and Notes

1. S. A. Bowring, I. S. Williams, *Contrib. Mineral. Petrol.* **134**, 3 (1999).
2. S. A. Wilde, J. W. Valley, W. H. Peck, C. M. Graham, *Nature* **409**, 175 (2001).
3. M. Boyet *et al.*, *Earth Planet. Sci. Lett.* **214**, 427 (2003).
4. G. Caro, B. Bourdon, J. Birck, S. Moorbath, *Nature* **423**, 428 (2004).
5. M. Boyet, R. W. Carlson, *Earth Planet. Sci. Lett.* **250**, 254 (2006).
6. G. Caro, B. Bourdon, J. Birck, S. Moorbath, *Geochim. Cosmochim. Acta* **70**, 164 (2006).
7. V. C. Bennett, A. D. Brandon, A. P. Nutman, *Science* **318**, 1907 (2007).
8. J. O'Neil *et al.*, in *In Earth's Oldest Rocks*, M. van Kranendonk, R. H. Smithies, V. C. Bennett, Eds. (Elsevier, Amsterdam, 2007), pp. 219–250.
9. J. David, L. Godin, R. K. Stevenson, J. O'Neil, D. Francis, *Geol. Soc. Am. Bull.*, in press (available at www.gsajournals.org/perlserv/?request=get-abstract&doi=10.1130%2FB26369.1).
10. M. Simard, M. Parent, J. David, K. N. M. Sharma, "Géologie de la région de la rivière Innuksuac (34K et 34L)" (Ministère des Ressources naturelles, RG 2002-10, Québec, Canada, 2003).
11. N. L. Cates, S. J. Mojzsis, *Earth Planet. Sci. Lett.* **255**, 9 (2007).
12. M. Boyet, R. W. Carlson, *Science* **309**, 576 (2005); published online 16 June 2005 (10.1126/science.1113634).
13. G. W. Lugmair, S. J. G. Galer, *Geochim. Cosmochim. Acta* **56**, 1673 (1992).
14. Y. Amelin, A. N. Krot, I. D. Hutcheon, A. A. Ulyanov, *Science* **297**, 1678 (2002).
15. D. J. DePaolo, *Nature* **291**, 193 (1981).
16. S. L. Goldstein, R. K. O'Nions, P. J. Hamilton, *Earth Planet. Sci. Lett.* **70**, 221 (1984).
17. V. C. Bennett, A. P. Nutman, M. T. McCulloch, *Earth Planet. Sci. Lett.* **119**, 299 (1993).
18. M. T. McCulloch, V. C. Bennett, *Geochim. Cosmochim. Acta* **58**, 4717 (1994).
19. M. T. McCulloch, V. C. Bennett, in *The Earth's Mantle*, I. Jackson, Ed. (Cambridge Univ. Press, Cambridge, 1998), pp. 127–158.
20. This research was supported by National Science and Engineering Research Council of Canada (NSERC) Discovery grants to D.F. (RGPIN 7977-00). We thank the municipality of Inukjuak and the Pituvik Landholding Corporation for permission to work on their territory; J. Mina, M. Carroll, V. Inukpuk Morkill, R. Kasudluak, and J. Williams for their hospitality and support; and M. Horan and T. Mock for analytical support. The Department of Terrestrial Magnetism Thermo-Fisher Scientific Triton (Bremen, Germany) was purchased with partial support from the NSF grant EAR-0320589.

Infants' Perseverative Search Errors Are Induced by Pragmatic Misinterpretation

József Topál,[1]* György Gergely,[1,2] Ádám Miklósi,[3] Ágnes Erdőhegyi,[3] Gergely Csibra[2,4]

Having repeatedly retrieved an object from a location, human infants tend to search the same place even when they observe the object being hidden at another location. This perseverative error is usually explained by infants' inability to inhibit a previously rewarded search response or to recall the new location. We show that the tendency to commit this error is substantially reduced (from 81 to 41%) when the object is hidden in front of 10-month-old infants without the experimenter using the communicative cues that normally accompany object hiding in this task. We suggest that this improvement is due to an interpretive bias that normally helps infants learn from demonstrations but misleads them in the context of a hiding game. Our finding provides an alternative theoretical perspective on the nature of infants' perseverative search errors.

Human infants' abilities for understanding the physical world are often tested in hide-and-search tasks. First demonstrated by Piaget (*1*), the perseverative search error (some-times called the A-not-B error) is a well-known and robust mistake that infants close to 1 year of age normally commit. In the standard A-not-B task, a demonstrator repeatedly places an object